

Sparse Principal Component Analysis via Rotation and Truncation

Zhenfang Hu^{*}, Gang Pan^{*}, Yueming Wang[†], and Zhaohui Wu^{*}

^{*}College of Computer Science and Technology, Zhejiang University, China,
zhenfhu@gmail.com, gpan@zju.edu.cn, zjuwuzh@gmail.com

[†]Qiushi Academy for Advanced Studies, Zhejiang University, China,
ymingwang@zju.edu.cn

March 18, 2019

Abstract

Sparse principal component analysis (sparse PCA) aims at finding a sparse basis to improve the interpretability over dense basis of PCA, meanwhile reflecting the data distribution. In contrast to most of existing work which deal with the problem by adding some sparsity penalties on various objectives of PCA, in this paper, we propose a new method SPCArt, whose motivation is to find a rotation matrix and a sparse basis such that the sparse basis approximates the basis of PCA after the rotation. The algorithm of SPCArt consists of three alternating steps: rotate PCA loadings, truncate small entries, and update the rotation matrix. Its performance bounds are also given. SPCArt is efficient, with each iteration scaling linearly with the data dimension. It is easy to choose parameters in SPCArt, due to its explicit physical explanations. Besides, we give a unified view to several existing sparse PCA methods and discuss the connection with SPCArt. Some ideas in SPCArt are extended to GPower, a popular sparse PCA algorithm, to overcome its drawback. Experimental results demonstrate that SPCArt achieves the state-of-the-art performance. It also achieves a good tradeoff among various criteria, including sparsity, explained variance, orthogonality, balance of sparsity among loadings, and computational speed.

Keywords: sparse, principal component analysis, rotation, truncation.

1 Introduction

In most research areas, the data we encountered are usually of very high dimensions, for examples, signal processing, machine learning, computer vision, document processing, computer network, and genetics etc. However, almost all data in the areas have much lower intrinsic dimensions. Thus, how to handle these data is a traditional problem.

1.1 PCA

Principal component analysis (PCA) [1] is one of the most popular analysis tools to deal with this situation. Given a set of data, whose mean is removed, PCA approximates the data by representing them in another orthonormal basis, called loading vectors. The coefficients of the data when represented using these loadings are called principal components. They are obtained by projecting the data onto the loadings, i.e. inner products between loading vectors and data vector. Usually, the loadings are deemed as a set of ordered vectors, in that the variances of data explained by them are in a decreasing order, e.g. the leading loading points to the maximal-variance direction. If the data lie in a low dimensional subspace, i.e. the distribution mainly varies in a few directions, a few loadings are enough to obtain a good approximation; and the original high-dimensional data now can be represented by the low-dimensional principal components, so dimensionality reduction is achieved.

Commonly, the dimensions of original data have some physical explanations. For example, in financial or biological applications, each dimension may correspond to a specific asset or gene [2]. However, the loadings obtained by PCA are usually dense, so the principal component is a mixture of all dimensions, which makes it difficult to interpret. If most of the entries in the loadings are zeros (sparse), each principal component becomes a linear combination of a few non-zero entries. This facilitates the understanding of the physical meaning of the loadings as well as the principal components. Further, the physical interpretation would be clearer if different loadings have different non-zero entries, i.e. corresponding to different dimensions.

1.2 Sparse PCA

Sparse PCA aims at finding a sparse basis to make the result more interpretable [3]. At the same time, the basis is required to represent the data distribution faithfully. Thus, there is a tradeoff between the statistical fidelity and the interpretability.

During the past decade, a variety of methods for sparse PCA have been proposed. Most of them have considered the tradeoff between sparsity and explained variance. However, there are three points that have not received enough attentions yet: the orthogonality between every two loadings, the balance of sparsity among loadings, and the global property of solution.

- Orthogonality. One advantage of PCA is that the loadings are orthogonal; but in the case of sparse PCA, this is not easy to satisfy. The orthogonality property is highly important since it indicates the independence of physical meaning of the loadings. When loadings are sufficiently sparse, orthogonality usually implies non-overlapping of their supports. So each loading represents distinctive physical meaning.
- Balance of sparsity. The balance of sparsity requires that the sparsity between different loadings should be as even as possible. That is, both leading loadings and the rest loadings should be sparse in a similar degree. In some approaches, the leading loadings are highly dense while the rest ones are sparse. This is unreasonable since the data distribution is mainly represented by the dense loadings, while the sparsity is primarily contributed by the rest less important loadings, which is indeed not helpful for physical explanations.
- Global property. The global property concerns whether the solution of a sparse PCA method is optimal enough. For a method, if the globally optimal solution or a solution close to the global optimal one can be computed, we say its “global property” is good. Otherwise, the global property of the method is not good. Usually, there are two types of methods for computing sparse loadings in existing work. One computes loadings one by one in a greedy manner, called deflation scheme [4]. The other finds all loadings simultaneously, called block scheme. The block scheme is better than the deflation one since the solutions of the former seem more “global” compared with the latter.

1.3 Our Method: SPCArt

In this paper, we propose a new approach called SPCArt (Sparse PCA via rotation and truncation). In contrast to most of traditional work which are based on adding some sparsity penalty on the objective of PCA, the motivation of SPCArt is distinctive. SPCArt aims to find a rotation matrix and a sparse basis such that the sparse basis approximates the loadings of PCA after the rotation. The resulting algorithm consists of three alternative steps: rotate PCA loadings, truncate small entries of them, and update the rotation matrix.

SPCArt has the following merits. (1) It is able to explain as much variance as the PCA loadings, since the sparse basis spans almost the same subspace as the PCA loadings. (2) The new basis is close to orthogonal, since it approximates the rotated PCA loadings. (3) The truncation tends to produce more balanced sparsity, since vectors of the rotated PCA loadings are of equal length. (4) It is less greedy and the solution tends to be more globally optimal compared with the deflation schemes, since SPCArt belongs to the block scheme.

The contributions of this paper are four-fold: (1) we propose an efficient algorithm SPCArt achieving good performance over a series of criteria, some of which have been overlooked by previous work; (2) we

Table 1: Time complexities for computing r loadings from n samples of dimension p . The preprocessing and initialization overheads are omitted. For PathSPCA, k is the cardinality of a loading. ST and SPCArt have the additional cost of initialization as PCA. The complexities of SPCArt listed below are with the truncation methods of T- ℓ_0 and T- ℓ_1 . Those of T-sp and T-en are $O(rp \log p + r^2 p + r^3)$.

	PCA [1]	ST [5]	SPCA [6]	PathSPCA [2]	ALSPCA [7]	GPower [8], rSVD-GP, TPower [9]	GPowerB [8], rSVD-GPB	SPCArt
$n > p$	$O(np^2)$	$O(rp)$	$O(r^2 p + rp^3)$	$O(rkp^2 + rk^3)$	$O(rp^2)$	$O(rp^2)$	$O(rpn + r^2 n)$	$O(r^2 p + r^3)$
$n < p$	$O(pn^2)$	$O(rp)$	$O(r^2 p + rnp)$	$O(rknp + rk^3)$	$O(rnp)$	$O(rnp)$	$O(rpn + r^2 n)$	$O(r^2 p + r^3)$

devise various truncation operations in SPCArt for different situations and provide performance analysis; (3) we give a unified view for a series of previous sparse PCA approaches, together with ours; (4) under the unified view, we find the relation between GPower, rSVD, and our method, and extend GPower and rSVD to a new version, called rSVD-GP, to overcome their drawbacks—parameter tuning problem and imbalance of sparsity among loadings.

The rest of the paper is organized as follows: Section 2 introduces representative work on sparse PCA. Section 3 presents the detail of our method SPCArt and the types of truncation operations, and analyzes their performance. Section 4 gives a unified view for a series of previous work. Section 5 shows the relation between GPower, rSVD, and our method, and extends GPower and rSVD to a new implementation, called rSVD-GP. Experimental results are provided in Section 6. Finally, we conclude this paper in Section 7.

2 Related Work

Various sparse PCA methods have been proposed during the past decade. We give a brief review of previous work below.

1) *Ad-hoc methods*. In early days, some ad-hoc methods were studied, in which loadings of PCA are post-processed to improve interpretability. For example, in [10] various rotations were applied to the loadings; and in [5] simple thresholding method (ST) was used to set the entries smaller than a small threshold to zero.

2) *Covariance matrix maximization*. More recently, systematic approaches based on solving explicit objectives were proposed, starting from SCoTLASS [3] which optimizes the classical objective of PCA, i.e. maximizing the quadratic form of covariance matrix, while additionally imposing a sparsity constraint on each loading.

3) *Matrix approximation*. SPCA [6] formulates the problem as a regression-type optimization, so as to facilitate the use of LASSO [11] or elastic-net [12] techniques to solve the problem. rSVD [13] and SPC [14] obtain sparse loadings by solving a sequence of rank-1 matrix approximations, with sparsity penalty or constraint imposed.

4) *Semidefinite convex relaxation*. Most of the methods proposed so far are local ones, which suffer from getting trapped in local minima. DSPCA [15] transforms the problem into a semidefinite convex relaxation problem, thus global optimality of solution is guaranteed. This distinguishes it from most of the other local methods. Unfortunately, its computational complexity is as high as $O(p^4 \sqrt{\log p})$ (p is the number of variables), which is expensive for most applications. Later, a variable elimination method [16] of complexity $O(p^3)$ was developed in order to make the application on large scale problem feasible.

5) *Greedy methods*. In [17], the authors used greedy search and branch-and-bound methods to solve small instances of the problem exactly. Each step of the algorithm has a complexity $O(p^3)$, leading to a total complexity of $O(p^4)$ for a full set of solutions (solutions of cardinality ranging from 1 to p). Later, this bound is improved in the classification setting [18]. In another way, a greedy algorithm PathSPCA [2] was presented to further approximate the solution process of [17], resulting in a complexity of $O(p^3)$ for a full set of solutions. For a review of DSPCA, PathSPCA, and their applications, see [19].

6) *Power methods*. The GPower method [8] formulates the problem as maximization of a convex objective function and the solution is obtained by generalizing the power method [20] to compute PCA

loadings. Recently, a new power method TPower [9], and a somewhat different but related power method ITSPCA [21] that aims at recovering sparse principal subspace, are proposed.

7) *Augmented lagrangian optimization.* In [7], a method called ALSPCA was proposed, which is based on an augmented lagrangian optimization and the solution is obtained by simultaneously considering the following factors: explained variance, orthogonality and correlation among principal components.

Among them only SCoTLASS [3] and ALSPCA [7] have considered the orthogonality of sparse loadings; and DSPCA [15] has considered the global property of solution.

The computational complexities of some of the above algorithms are summarized in Table 1.

3 SPCArt: Sparse PCA via Rotation and Truncation

In this section, we first give a brief overview of SPCArt, next introduce the detailed formulation, and then introduce different truncation types, and finally provide performance analysis.

The idea behind SPCArt can be understood as follows. Since any rotation of the r PCA loadings $[V_1, \dots, V_r] \in \mathbb{R}^{p \times r}$ constitutes an orthogonal basis spanning the same subspace, $X = VR$ ($R \in \mathbb{R}^{r \times r}$, $R^T R = I$), we want to find a rotation matrix R through which V is transformed to a sparsest basis X . It is difficult to solve this problem directly, so instead we would find a rotation matrix and a sparse basis such that the sparse basis approximates the PCA loadings after the rotation. Roughly, the objective function takes the form of: $\min_{X,R} \|V - XR\|_F^2 + \lambda \|X\|_0$, where $\|\cdot\|_0$ is a sparsity penalty.

The above problem is solved by alternatively fixing one variable and optimizing the other. Both the two subproblems have closed-form solutions. There are three steps in solving the problem: 1) rotate V to a new basis $Z = VR^T$; 2) truncate Z to a sparse X ; 3) update R via the polar decomposition of $X^T V$. Four types of truncations are designed to deal with different situations, including hard thresholding (T- ℓ_0), soft thresholding (T- ℓ_1), truncation by energy percentage (T-en), and truncation by sparsity (T-sp). For each type, performance analysis is provided.

3.1 Formulation of SPCArt

Our method is motivated by the solution of Eckart-Young theorem [22]. This theorem is well-known in numerical linear algebra. It is concerned with the problem of approximating a matrix by a low-rank one.

Theorem 1. (Eckart-Young Theorem) Assume the SVD of a matrix $A \in \mathbb{R}^{n \times p}$ is $A = U\Sigma V^T$, in which $U \in \mathbb{R}^{n \times m}$, $m \leq \min\{n, p\}$, $\Sigma \in \mathbb{R}^{m \times m}$ is diagonal with $\Sigma_{11} \geq \Sigma_{22} \geq \dots \geq \Sigma_{mm}$, and $V \in \mathbb{R}^{p \times m}$. A rank r ($r \leq m$) approximation of A is to solve the following problem:

$$\min_{Y,X} \|A - YX^T\|_F^2, \text{ s.t. } X^T X = I, \quad (1)$$

where $Y \in \mathbb{R}^{n \times r}$ and $X \in \mathbb{R}^{p \times r}$. A solution is

$$X^* = V_{1:r}, Y^* = AX^*, \quad (2)$$

where $V_{1:r}$ is the first r columns of V .

Alternatively, the solution can be expressed as

$$Y^* = U_{1:r}\Sigma_{1:r}, X^* = \text{Polar}(A^T Y^*), \quad (3)$$

where $\text{Polar}(\cdot)$ is defined as follows [8]. Given a matrix $Z \in \mathbb{R}^{n \times p}$, $n > p$, and $Z = WS$ where $W \in \mathbb{R}^{n \times p}$ is orthonormal and $S \in \mathbb{R}^{p \times p}$ is positive semidefinite, then $\text{Polar}(Z) = W$. If the thin SVD of Z is $U\Sigma V^T$, then $W = UV^T$, $S = V\Sigma V^T$, and

$$\text{Polar}(Z) = UV^T. \quad (4)$$

Note that if each column of A has been centered to have mean zero, $V_{1:r}$ are the loadings obtained by PCA. Clearly, $\forall R \in \mathbb{R}^{r \times r}$ and $R^T R = I$, $X^* = V_{1:r}R$ and $Y^* = AX^* = U_{1:r}\Sigma_{1:r}R$ is also a solution of (1). This implies that any rotation of the r orthonormal leading eigenvectors $V_{1:r} \in \mathbb{R}^{p \times r}$ is a solution of

the best rank r approximation of A . That is, any orthonormal basis in the corresponding eigen-subspace is capable of representing the original data distribution as well as the original basis. Thus, a natural idea for sparse PCA is to find a rotation matrix R so that $X = V_{1:r}R$ becomes sparse, i.e.,

$$\min_{R \in \mathbb{R}^{r \times r}} \|V_{1:r}R\|_0, \text{ s.t. } R^T R = I, \quad (5)$$

where $\|\cdot\|_0$ denotes the sum of ℓ_0 norm of the columns of a matrix. For sparse problems, the ℓ_1 norm is a widely-used convex surrogate of the ℓ_0 norm:

$$\min_{R \in \mathbb{R}^{r \times r}} \|V_{1:r}R\|_1, \text{ s.t. } R^T R = I, \quad (6)$$

where $\|\cdot\|_1$ denotes the sum of ℓ_1 norm of the columns of a matrix.

Unfortunately, both of the above two problems are hard to solve. So we approximate them instead. Since $X = V_{1:r}R \Leftrightarrow V_{1:r} = XR^T$, we want to find a rotation matrix R through which a sparse basis X approximates original PCA loadings. Without confusion, we use V to denote $V_{1:r}$ hereafter. The ℓ_0 version is

$$\min_{X,R} \|V - XR\|_F^2 + \lambda^2 \sum_i \|X_i\|_0, \text{ s.t. } R^T R = I, \quad (7)$$

and the ℓ_1 version is

$$\begin{aligned} \min_{X,R} \frac{1}{2} \|V - XR\|_F^2 + \lambda \sum_i \|X_i\|_1, \\ \text{s.t. } \forall i, \|X_i\|_2 = 1, R^T R = I. \end{aligned} \quad (8)$$

If the approximation is accurate enough, i.e., $V \approx XR$, then $X \approx VR^T$ would be near orthogonal and explain similar variance as V . Note that both (7) and (8) exhibit to be matrix approximation problems as (1) in the Eckart-Young theorem. The key difference is that there are sparsity penalties in (7) and (8). But the solutions still share some common features.

There are two matrix variables in the above problems, R and X . It is difficult to solve them simultaneously. So we solve the problems by fixing one and optimizing the other alternately. Both the subproblems have closed-form solutions.

When X is fixed, both of (7) and (8) become a Procrustes problem [6]:

$$\min_R \|V - XR\|_F^2, \text{ s.t. } R^T R = I. \quad (9)$$

We have a solution $R^* = \text{Polar}(X^T V)$, where $\text{Polar}(\cdot)$ is defined in (4). The solution is of the same form as (3).

When R is fixed, (8) becomes

$$\min_X \frac{1}{2} \|VR^T - X\|_F^2 + \lambda \sum_i \|X_i\|_1, \text{ s.t. } \forall i, \|X_i\|_2 = 1. \quad (10)$$

It can be divided into r independent subproblems, one for each column: $\min_{X_i} 1/2 \|Z_i - X_i\|_2^2 + \lambda \|X_i\|_1, \text{ s.t. } \|X_i\|_2 = 1$, where $Z = VR^T$. It is equivalent to $\max_{X_i} Z_i^T X_i - \lambda \|X_i\|_1, \text{ s.t. } \|X_i\|_2 = 1$. The solution is $X_i^* = S_\lambda(Z_i) / \|S_\lambda(Z_i)\|_2$ [8], where $S_\lambda(\cdot)$ denotes entry-wise soft thresholding

$$S_\lambda(x) = \text{sign}(x)(|x| - \lambda)_+, \quad x \in \mathbb{R}, \quad (11)$$

in which $[y]_+ = y$ if $y \geq 0$ and $[y]_+ = 0$ otherwise.

Still fixing R , (7) becomes

$$\min_X \|VR^T - X\|_F^2 + \lambda^2 \sum_i \|X_i\|_0. \quad (12)$$

Let $Z = VR^T$. There are also r subproblems: $\min_{X_i} \|Z_i - X_i\|_2^2 + \lambda^2 \|X_i\|_0$. It can be further decomposed to entry-wise problems and if $|Z_{ij}| \leq \lambda$, then $X_{ij}^* = 0$, otherwise $X_{ij}^* = Z_{ij}$. Hence the solution can be expressed as $X_i^* = H_\lambda(Z_i)$, where $H_\lambda(\cdot)$ denotes entry-wise hard thresholding

$$H_\lambda(x) = x[\text{sign}(|x| - \lambda)]_+, \quad x \in \mathbb{R}, \quad (13)$$

Algorithm 1 SPCArt

- 1: **Input:** A data matrix $A \in \mathbb{R}^{n \times p}$ containing n samples with the dimension of p , the number of loadings r , the truncation type T , and the truncation parameter λ .
 - 2: **Output:** sparse loading vectors $\{X_1, \dots, X_r\}$, arranged column-wise in matrix $X \in \mathbb{R}^{p \times r}$.
 - 3: PCA: compute rank r SVD of A : $U\Sigma V^T$, $V \in \mathbb{R}^{p \times r}$.
 - 4: Initialize R : $R = I$.
 - 5: **repeat**
 - 6: Rotation: $X = VR^T$
 - 7: Truncation:
 - 8: **switch** T
 - 9: **case** T- ℓ_0 : $\forall i, j$, if $|X_{ji}| < \lambda$ set $X_{ji} = 0$.
 - 10: **case** T- ℓ_1 : $\forall i, j$, $X_{ji} = \text{sign}(X_{ji}) \cdot \max(|X_{ji}| - \lambda, 0)$
 - 11: **case** T-en: $\forall i$, \bar{X}_i is sorted $|X_i|$ in ascending order. Find $k = \text{argmax}_t t$, s.t. $\sum_{j=1}^t \bar{X}_{ji}^2 \leq \lambda$, and set entries of X_i associated with the first k entries of \bar{X}_i to 0.
 - 12: **case** T-sp: $\forall i$, set the smallest λ entries (in absolute value) of X_i to 0.
 - 13: **end**
 - 14: Normalize X : $\forall i$, $X_i = X_i / \|X_i\|_2$.
 - 15: Update R : compute SVD of $X^T V$: WDQ^T , $R = WQ^T$.
 - 16: **until** termination condition
-

where $H_\lambda(x) = 0$ if $|x| \leq \lambda$, $H_\lambda(x) = x$ otherwise.

Note that there is no normalization for X^* in this case compared with the ℓ_1 case. This is because if unit length constraint $\|X_i\|_2 = 1$ is added to (7), there will be no closed form solutions. We still let $X_i^* = H_\lambda(Z_i) / \|H_\lambda(Z_i)\|_2$ for consistency, since practically no significant difference is observed.

In both cases, truncations are conducted to produce sparsity. Because of the unit length of each column vector in Z , a single threshold $0 \leq \lambda < 1$ is feasible to make the sparsity to distribute evenly between the vectors. Otherwise we have to apply different thresholds for different columns which are difficult to determine. Since Z is a rotation of the original eigen-basis V , it is orthonormal. On the other hand, X^* is obtained via truncating small entries of Z , so X is still possible to be a near-orthogonal basis. This is the basic model of our method, called SPCArt.

The computational complexity of SPCArt is shown in the last column of Table 1. Except the computational cost of PCA loadings, SPCArt scales linearly about data dimension. When the number of loadings is not too large, it is efficient.

3.2 Truncation Types

In this section, we discuss the different truncation types. Four types of truncations are devised, including T- ℓ_1 soft thresholding, T- ℓ_0 hard thresholding, T-en truncation, and T-sp truncation. The soft thresholding T- ℓ_1 and hard thresholding T- ℓ_0 have been defined in (11) and (13), and the other two truncation types are introduced below.

Note that both ℓ_0 and ℓ_1 penalties only result in thresholding operation on Z and nothing else. Hence, we could devise other truncation types irrespective of explicit objective:

T-en: truncation by energy percentage. T-en truncates and normalizes X_i by $X_i = E_\lambda(Z_i) / \|E_\lambda(Z_i)\|_2$, where λ is the percentage of energy, $0 \leq \lambda < 1$, $\forall X \in \mathbb{R}^p$, $\|X\|_2 = 1$, and the operation $E_\lambda(X)$ truncates the smallest entries of X whose energy take up λ percentage. In practice, sort $\{|X_1|, \dots, |X_p|\}$ in ascending order to be $\{\bar{X}_1, \dots, \bar{X}_p\}$ and find $k = \text{argmax}_i i$, s.t. $\sum_{j=1}^i \bar{X}_j^2 \leq \lambda$, then set entries of X associated with the first k entries of \bar{X} to 0.

T-sp: truncation by sparsity. T-sp truncates and normalizes X_i by $X_i = P_\lambda(Z_i) / \|P_\lambda(Z_i)\|_2$, $\lambda \in \{0, 1, \dots, p-1\}$. $\forall X \in \mathbb{R}^p$, $P_\lambda(X)$ truncates the smallest λ entries of X . It corresponds to the ℓ_0 constrained objective, see (30).

The complete algorithm of SPCArt with all types of truncations is shown in Algorithm 1. When using T- ℓ_0 , the first iteration of SPCArt, i.e. $X_i = H_\lambda(V_i)$, corresponds to the ad-hoc simple thresholding

method ST [5], which is frequently used in practice and sometimes produced good results [6, 17]. Our SPCArt systematically promotes the seminal ideas of factor rotation [10] and simple thresholding [5].

3.3 Performance Analysis

This section discusses how performance in our method is guaranteed. For $X_i = T_\lambda(Z_i)/\|T_\lambda(Z_i)\|_2$, $i = 1, \dots, r$, where $Z = [Z_1, \dots, Z_r] \in \mathbb{R}^{p \times r}$, $p > r$, contains orthonormal columns, $X = [X_1, \dots, X_r] \in \mathbb{R}^{p \times r}$ is sparse output, and $T_\lambda(\cdot)$ is one of the four truncation types given in the previous section, we study the following problems: given threshold λ ,

- (1) How much sparsity of X_i can SPCArt achieved?
- (2) How much deviation does X_i have from Z_i ?
- (3) How much orthogonality is there between the columns of X ?
- (4) How many variances are explained by X ?

We first formulate performance bounds as functions of parameter λ . Then according to these bounds, we can explicitly control sparsity, orthogonality and explained variance via λ . First of all, we give some definitions as follows.

Definition 2. $\forall x \in \mathbb{R}^p$, the **sparsity** of x is the proportion of zero entries: $s(x) = 1 - \|x\|_0/p$.

Definition 3. $\forall z \in \mathbb{R}^p$, $z \neq 0$, $x = T_\lambda(z)/\|T_\lambda(z)\|_2$, the **deviation** of x from z is $\sin(\theta(x, z))$, where $\theta(x, z)$ is the included angle between x and z , $0 \leq \theta(x, z) \leq \pi/2$. If $x = 0$, $\theta(x, y)$ is defined to be $\pi/2$.

Definition 4. $\forall x, y \in \mathbb{R}^p$, $x \neq 0$, $y \neq 0$, the **nonorthogonality** between x and y is $|\cos(\theta(x, y))| = |x^T y|/(\|x\|_2 \cdot \|y\|_2)$, where $\theta(x, y)$ is the included angle between x and y .

Definition 5. Given data matrix $A \in \mathbb{R}^{n \times p}$ containing n samples of dimension p , \forall basis $X \in \mathbb{R}^{p \times r}$, $r \leq p$, the **explained variance** by X to A is $EV(X) = \text{tr}(X^T A^T A X)$. Let U be any orthonormal basis in the subspace spanned by X , then the **cumulative percentage of explained variance** is $CPEV(X) = \text{tr}(U^T A^T A U)/\text{tr}(A^T A)$ [13].

Intuitively, a larger threshold λ leads to higher sparsity. The same can be found for the deviation. When two truncated vectors deviate from the original orthogonal vectors, in the worst case, the nonorthogonality of them degenerates as the ‘sum’ of their deviations. On the other side, if the deviations of a sparse basis from the rotated loadings are small, we expect the sparse basis still represents data well, and the explained variance or cumulative percentage of explained variance maintains similar level to that of PCA. So, both the nonorthogonality and the explained variance depend on the deviations, and the deviation and sparsity are controlled by λ . We now go into details. The proofs of some of the following results are included in Appendix A.

3.3.1 Orthogonality

First, we have relative upper bound on nonorthogonality.

Proposition 6. $\forall z_1, z_2 \in \mathbb{R}^p$, $z_1 \perp z_2$. If $x_1 = T_{\lambda_1}(z_1)$, $x_2 = T_{\lambda_2}(z_2)$, then nonorthogonality

$$|\cos(\theta(x_1, x_2))| \leq \begin{cases} \sin(\theta(x_1, z_1) + \theta(x_2, z_2)) & , \theta(x_1, z_1) + \theta(x_2, z_2) \leq \pi/2, \\ 1 & , \text{otherwise.} \end{cases} \quad (14)$$

The bounds can be obtained by considering the two conical surfaces generated by axes z_i with rotational angles $\theta(x_i, z_i)$. So the nonorthogonality is determined by the sum of deviated angles. When the deviations are small, which depends on λ , then good orthogonality can be obtained.

3.3.2 Sparsity and Deviation

$\forall z \in \mathbb{R}^p$, $\|z\|_2 = 1$, $x = T_\lambda(z)/\|T_\lambda(z)\|_2$, we derive bounds about sparsity $s(x)$, and deviation $\sin(\theta(x, z))$ for each T . They depend on a key value $1/\sqrt{p}$, which is the entry value of a uniform vector of unit length.

Proposition 7. For T - ℓ_0 (13), the sparsity bounds are

$$\begin{cases} 0 \leq s(x) \leq 1 - \frac{1}{p} & , \lambda < \frac{1}{\sqrt{p}}, \\ 1 - \frac{1}{p\lambda^2} \leq s(x) \leq 1 & , \lambda \geq \frac{1}{\sqrt{p}}. \end{cases} \quad (15)$$

Deviation $\sin(\theta(x, z)) = \|\bar{z}\|_2$, where \bar{z} is the truncated part: $\bar{z}_i = z_i$ if $x_i = 0$, and $\bar{z}_i = 0$ otherwise. The absolute bounds are:

$$0 \leq \sin(\theta(x, z)) \leq \begin{cases} \sqrt{p-1}\lambda & , \lambda < \frac{1}{\sqrt{p}}, \\ 1 & , \lambda \geq \frac{1}{\sqrt{p}}. \end{cases} \quad (16)$$

All the above bounds are achievable.

Because when $\lambda < 1/\sqrt{p}$, there is no sparsity guarantee, λ is usually set to be $1/\sqrt{p}$ in practice. Generally it works well.

Proposition 8. For T - ℓ_1 (11), the bounds of $s(x)$ and lower bound of $\sin(\theta(x, z))$ are the same as T - ℓ_0 . In addition, there are relative deviation bounds

$$\|\bar{z}\|_2 \leq \sin(\theta(x, z)) < \sqrt{\|\bar{z}\|_2^2 + \lambda^2\|x\|_0}. \quad (17)$$

By the relative lower bounds, we have

Corollary 9. The deviation due to soft thresholding is always larger than that of hard thresholding $\sin_{S_\lambda}(\theta(x, z)) \geq \sin_{H_\lambda}(\theta(x, z))$, if the same λ is applied.

This implies that results got by T - ℓ_1 have potentially greater sparsity and less explained variance than those of T - ℓ_0 .

Proposition 10. For T -en, $0 \leq \sin(\theta(x, z)) \leq \sqrt{\lambda}$. Usually, $\sin(\theta(x, z)) \approx \sqrt{\lambda}$. In addition

$$\lfloor \lambda p \rfloor / p \leq s(x) \leq 1 - 1/p. \quad (18)$$

If $\lambda < 1/p$, there is no sparsity guarantee. When p is moderately large, $\lfloor \lambda p \rfloor / p \approx \lambda$.

Due to discrete nature of the operand, the actually truncated energy can be less than λ . But in practice, especially when p is moderately large, the effect is negligible. So we usually have $\sin(\theta(x, z)) \approx \sqrt{\lambda}$. Note that, the main advantage of T -en is that it has direct control on deviation. And recall that the deviation has direct influence on the nonorthogonality and the explained variance. Thus, if it is desirable to gain specific orthogonality and explained variance, T -en is preferable. Besides, when p is moderately large, T -en also gives nice control on sparsity.

Proposition 11. For T -sp, $\lambda/p \leq s(z) \leq 1$, the lower bound is usually achieved, and

$$0 \leq \sin(\theta(x, z)) \leq \sqrt{\lambda/p}. \quad (19)$$

The main advantage of T -sp lies in its direct control on sparsity. If we want to obtain specific sparsity, it can be applied.

3.3.3 Explained Variance

Finally, we derive bounds on the explained variance $EV(X) = \text{tr}(X^T A^T A X)$. Two results are provided. The first one is general and is applicable to any basis X not limited to sparse ones. The second one is tailored to SPCArt.

Theorem 12. *Let rank r SVD of $A \in \mathbb{R}^{n \times p}$ be $U\Sigma V^T$, $\Sigma \in \mathbb{R}^{r \times r}$. Given $X \in \mathbb{R}^{p \times r}$, assume SVD of $X^T V$ is $W D Q^T$, $D \in \mathbb{R}^{r \times r}$, $d_{\min} = \min_i D_{ii}$. Then*

$$d_{\min}^2 \cdot EV(V) \leq EV(X), \quad (20)$$

and $EV(V) = \sum_i \Sigma_{ii}^2$.

The theorem can be interpreted as follows. If X is a basis that approximates rotated PCA loadings well, then d_{\min} will be close to one, and so the variance explained by X is close to that explained by PCA. Note that variance explained by PCA loadings is the largest value that is possible to be achieved by orthonormal basis. Conversely, if X deviates much from the rotated PCA loadings, then d_{\min} tends to zero, so the variance explained by X is not guaranteed to be much. We see that the less the sparse loadings deviates from rotated PCA loadings, the more variance they explain.

When SPCArt converges, i.e. $X_i = T_\lambda(Z_i) / \|T_\lambda(Z_i)\|_2$, $Z \doteq V R^T$, and $R = \text{Polar}(X^T V)$ hold simultaneously, we have another estimation.

Theorem 13. *Let $C = Z^T X$, i.e. $C_{ij} = \cos(\theta(Z_i, X_j))$, and let \bar{C} be C with diagonal elements removed. Assume $\theta(Z_i, X_i) = \theta$ and $\sum_j C_{ij}^2 \leq 1$, $\forall i$, then*

$$(\cos^2(\theta) - \sqrt{r-1} \sin(2\theta)) \cdot EV(V) \leq EV(X). \quad (21)$$

When θ is sufficiently small,

$$(\cos^2(\theta) - O(\theta)) \cdot EV(V) \leq EV(X). \quad (22)$$

Since the sparse loadings are obtained by truncating small entries of the rotated PCA loadings, and θ is the deviation angle between these sparse loadings and the rotated PCA loadings, the theorem clearly implies, if the deviation is small then the variance explained by the sparse loadings is close to that of PCA, as $\cos^2(\theta) \approx 1$. For example, if the truncated energy $\|\bar{z}\|_2^2 = \sin^2(\theta)$ is about 0.05, then 95% EV of PCA loadings is guaranteed.

The assumptions $\theta(Z_i, X_i) = \theta$ and $\sum_j C_{ij}^2 \leq 1$, $\forall i$, are roughly satisfied by T-en using small λ . Uniform deviation $\theta(Z_i, X_i) = \theta$, $\forall i$, can be achieved by T-en as indicated by Proposition 10. $\sum_j C_{ij}^2 \leq 1$ means the sum of projected length is less than 1, when Z_i is projected onto each X_j . It is likely to be satisfied if X is near orthogonal, which can be achieved by setting small λ according to Proposition 6. In this case, about $(1 - \lambda)EV(V)$ is guaranteed.

Finally we mention that, in practice, we usually use the cumulative percentage of explained variance CPEV [13] rather than EV. CPEV measures the variance explained by subspace rather than basis. Since it is also the projected length of A onto the subspace spanned by X , the higher CPEV is, the better X represents data distribution. But when X is near orthogonal, EV is proportional to CPEV.

4 A Unified View to Some Prior Work

Though they may be proposed independently and formulated in various forms originally, a series of methods: PCA [1], SCoTLASS [3], SPCA [6], GPower [8], rSVD [13], TPower [9], SPC [14], and SPCArt can be derived from the common source of Theorem 1, the Eckart-Young Theorem. Most of them can be seen as the problems of matrix approximation (1), with different sparsity penalties. Most of them have two matrix variables, and the solution of them usually can be obtained by an alternating scheme: fix one and solve the other. Similar to SPCArt, the two subproblems are a sparsity penalized/constrained regression problem and a Procrustes problem.

PCA [1]. Since $Y^* = AX^*$, substituting $Y = AX$ into (1) and optimizing X , the problem (1) becomes,

$$\max_X \text{tr}(X^T A^T A X), \text{ s.t. } X^T X = I. \quad (23)$$

The solution is $X^* = V_{1:r}R$, $\forall R^T R = I$. If A has been centered to have mean zero, the special solution $X^* = V_{1:r}$ are exactly the r loadings obtained by PCA.

SCoTLASS [3]. Constraining X to be sparse in (23), we get SCotLASS,

$$\max_X \text{tr}(X^T A^T A X), \text{ s.t. } X^T X = I, \forall i, \|X_i\|_1 \leq \lambda. \quad (24)$$

The problem is not easy to solve.

SPCA [6]. If we substitute $Y = AX$ into (1) and separate the two X 's into two independent variables X and Z , in which Z subjects to a sparse constraint, we get SPCA,

$$\begin{aligned} \min_{Z, X} & \|A - AZX^T\|_F^2 + \lambda \|Z\|_F^2 + \sum_i \lambda_{1i} \|Z_i\|_1, \\ \text{s.t. } & X^T X = I, \end{aligned} \quad (25)$$

where Z is treated as target sparse loadings and λ 's are weights. When X is fixed, the problem is equivalent to r elastic-net problems: $\min_{Z_i} \|AX_i - AZ_i\|_F^2 + \lambda \|Z_i\|_2^2 + \lambda_{1i} \|Z_i\|_1$. When Z is fixed, it is a Procrustes problem: $\min_X \|A - AZX^T\|_F^2$, $\text{s.t. } X^T X = I$, and $X^* = \text{Polar}(A^T AZ)$.

GPower [8]. This is an important method. The three methods rSVD, TPower and SPC below can be seen as special cases. Except some artificial factors, the original GPower deals with the following ℓ_0 and ℓ_1 versions of objectives:

$$\max_{Y, W} \sum_i (Y_i^T A W_i)^2 - \lambda_i \|W_i\|_0, \text{ s.t. } Y^T Y = I, \forall i, \|W_i\|_2 = 1, \quad (26)$$

$$\max_{Y, W} \sum_i Y_i^T A W_i - \lambda_i \|W_i\|_1, \text{ s.t. } Y^T Y = I, \forall i, \|W_i\|_2 = 1. \quad (27)$$

They can be seen as derived from the following more fundamental ones.

$$\min_{Y, X} \|A - YX^T\|_F^2 + \sum_i \lambda_i \|X_i\|_0, \text{ s.t. } Y^T Y = I, \quad (28)$$

$$\min_{Y, X} \frac{1}{2} \|A - YX^T\|_F^2 + \sum_i \lambda_i \|X_i\|_1, \text{ s.t. } Y^T Y = I. \quad (29)$$

More details can be found in Appendix B.

Further, these two objectives can be seen as derived from (1): a mirror version of Theorem 1 exists $\min_{Y, X} \|A - YX^T\|_F^2$, $\text{s.t. } Y^T Y = I$, where $A \in \mathbb{R}^{n \times p}$ is still seen as a data matrix containing n samples of dimension p . The solution is $X^* = V_{1:r} \Sigma_{1:r} R$ and $Y^* = \text{Polar}(AX^*) = U_{1:r} R$. Adding sparsity penalties to X , we get (28) and (29).

Following the alternating optimization scheme. When X is fixed, in both cases $Y^* = \text{Polar}(AX)$. When Y is fixed, the ℓ_0 case becomes $\min_X \|A^T Y - X\|_F^2 + \sum_i \lambda_i \|X_i\|_0$. Let $Z = A^T Y$, then $X_i^* = H_{\sqrt{\lambda_i}}(Z_i)$, where $H_\lambda(\cdot)$ is defined in (13); the ℓ_1 case becomes $\min_X 1/2 \|A^T Y - X\|_F^2 + \sum_i \lambda_i \|X_i\|_1$, $X_i^* = S_\lambda(Z_i)$, where $S_\lambda(\cdot)$ is defined in (11). The i th loading is obtained by normalizing X_i to the unit length.

The iterative steps combined together produce essentially the same solution processes to the original ones in [8]. But, the matrix approximation formulation makes the relation of GPower to SPCArt and methods below apparent.

rSVD [13]. rSVD can be seen as a special case of GPower, i.e. the single component case $r = 1$. Here $\text{Polar}(\cdot)$ reduces to unit length normalization. More loadings can be got via the *deflation* scheme [4, 13], e.g. update $A \leftarrow A(I - x^* x^{*T})$ and run the procedure again. Since $Ax^* = 0$, it indicates that the subsequent loadings are near orthogonal to x^* .

Further, in rSVD, if we replace the penalties with constraints, the methods become equivalent to TPower and SPC.

TPower [9]. For the ℓ_0 case, we solve

$$\min_{y \in \mathbb{R}^n, x \in \mathbb{R}^p} \|A - yx^T\|_F^2, \text{ s.t. } \|x\|_0 \leq \lambda, \|y\|_2 = 1. \quad (30)$$

Algorithm 2 rSVD-GP: deflation version

1: **Input:** data matrix $A = [A_1, \dots, A_p] \in \mathbb{R}^{n \times p}$ containing n samples of dimension p (or covariance matrix $C \in \mathbb{R}^{p \times p}$), number of loadings r , truncation type T , parameter λ .
2: **Output:** r sparse loading vectors $x_i \in \mathbb{R}^p$.
3: **for** $i = 1$ **to** r **do**
4: Initialize x_i : $j = \operatorname{argmax}_k \|A_k\|_2$ (or $j = \operatorname{argmax}_k C_{kk}$), set $x_{ij} = 1$, $x_{ik} = 0$, $\forall k \neq j$.
5: **repeat**
6: $z = A^T A x_i$ (or $z = C x_i$), $x_i = T_\lambda(z/\|z\|_2)$.
7: **until** termination condition met
8: Normalize X : $x_i = x_i/\|x_i\|_2$.
9: Deflation: $A = A(I - x_i x_i^T)$ (or $C = (I - x_i x_i^T)C(I - x_i x_i^T)$).
10: **end for**

The closed form solution is $y^* = Ax/\|Ax\|_2$ and $x^* = P_{p-\lambda}(A^T y)$. $\forall z \in \mathbb{R}^p$, $P_\lambda(z)$ sets the smallest (in absolute value) λ entries of z to zero¹. By iteration, $x^{(t+1)} \propto P_{p-\lambda}(A^T A x^{(t)})$, which indicates equivalence to the original TPower.

SPC [14]. Finally, for ℓ_1 case, we solve $\min_{y,d,x} \|A - ydx^T\|_F^2$, s.t. $\|x\|_1 \leq \lambda$, $\|y\|_2 = 1$, $\|x\|_2 = 1$, $d \in \mathbb{R}$. d serves as length of x in (30). When the other variables are fixed, $d^* = y^T A x$. when d is fixed, the problem is: $\max_{y,x} \operatorname{tr}(y^T A x)$, s.t. $\|x\|_1 \leq \lambda$, $\|y\|_2 = 1$, $\|x\|_2 = 1$. A small modification further leads to SPC:

$$\max_{y,x} \operatorname{tr}(y^T A x), \text{ s.t. } \|x\|_1 \leq \lambda, \|y\|_2 \leq 1, \|x\|_2 \leq 1.$$

This problem is biconvex and can be solved by linear searching, $y^* = Ax/\|Ax\|_2$. However, there is no analytic solution for x .

5 Relation of GPower to SPCArt and an Extension

5.1 Relation of GPower to SPCArt

Note that (28) and (29) are of similar forms to (7) and (8) respectively. There are two important points of differences. First, SPCArt deals with orthonormal eigenvectors rather than original data. Second, SPCArt takes rotation matrix rather than orthonormal matrix as variable. These differences are the key points for the success of SPCArt.

Compared with SPCArt, GPower has some drawbacks. GPower can work on both the deflation mode ($r = 1$, i.e. rSVD) and the block mode ($r > 1$). In the block mode, there is no mechanism to ensure the orthogonality of the loadings. Here $Z = A^T Y$ is not orthogonal, so after thresholding, X also does not tend to be orthogonal. Besides, it is not easy to determine the weights, since lengths of Z_i usually vary in great range. E.g., if we initialize $Y = U_{1:r}$, then $Z = A^T Y = V_{1:r} \Sigma_{1:r}$, which are scaled PCA loadings whose lengths usually decay exponentially. Thus, if we simply set the thresholds λ_i uniformly, it is easy to lead to unbalanced sparsity among loadings, in which leading loadings may be highly denser. This deviates from the goal of sparse PCA. For the deflation mode, though it produces near orthogonal loadings, the greedy scheme makes its solution less globally optimal. And there is still a problem of how to set the weights appropriately too.² Besides, for both modes, performance analysis may be difficult to obtain.

5.2 Extending rSVD and GPower to rSVD-GP

A major drawback of rSVD and GPower is that they can not use uniform thresholds when applying thresholding $x = T_\lambda(z)$. The problem does not exist in SPCArt since the inputs are of unit length. But, we can extend the similar idea to GPower and rSVD. Let $x = \|z\|_2 \cdot T_\lambda(z/\|z\|_2)$, which is equivalent to truncating z according to its length, or using adaptive thresholds $x = T_{\lambda\|z\|_2}(z)$. The other types of

¹[13] did implement this version for rSVD, but using a heuristic trick.

²Even if y is initialized with the maximum-length column of A as [8] does, it is likely to align with U_1 .

Algorithm 3 rSVD-GPB: block version

- 1: **Input:** data matrix $A \in \mathbb{R}^{n \times p}$ containing n samples of dimension p , number of loadings r , truncation type T , parameter λ .
 - 2: **Output:** sparse loading vectors $\{X_1, \dots, X_r\}$, arranged column-wise in matrix $X \in \mathbb{R}^{p \times r}$.
 - 3: PCA: compute rank r SVD of A : $Y\Sigma V^T$.
 - 4: **repeat**
 - 5: $Z = A^T Y$, $X_i = \|Z_i\|_2 \cdot T_\lambda(Z_i/\|Z_i\|_2)$, $\forall i$.
 - 6: Update Y : compute SVD of AX : WDQ^T , $Y = WQ^T$.
 - 7: **until** termination condition met
 - 8: Normalize X : $\forall i$, $X_i = X_i/\|X_i\|_2$.
-

truncations T-en and T-sp can be introduced into GPower too. T-sp is insensitive to length, so there is no trouble in parameter setting, and the deflation version is exactly TPower. The deflation version of the improved algorithm rSVD-GP is shown in Algorithm 2, and the block version rSVD-GPB is shown in Algorithm 3. In deflation case, it is more efficient to operate on covariance matrix, if $n > p$.

6 Experiments

The data sets used include: (1) a synthetic data with some underlying sparse loadings [6]; (2) the classical Pitprops data [23]; (3) a natural image data with moderate dimension and relatively large sample size, on which comprehensive evaluations are conducted; (4) a gene data with high dimension and small sample size [24]; (5) a set of random data with increasing dimensions for the purpose of speed test.

We compare our methods with five methods: SPCA [6], PathSPCA [2], ALSPCA [7], GPower [8], and TPower [9]. For SPCA, we use toolbox [25], which implements ℓ_0 and ℓ_1 constraint versions. We use GPowerB to denote the block version of GPower, as rSVD-GPB. We use SPCArt(T- ℓ_0) to denote SPCArt using T- ℓ_0 ; the other methods use the similar abbreviations. Note that, rSVD-GP(T-sp) is equivalent to TPower [9]. Except our SPCArt and rSVD-GP(B), the codes of the others are downloaded from the authors' websites.

There are mainly five criteria to assess the performance of algorithms. (1) SP: mean of sparsity of loadings. (2) STD: standard deviation of sparsity of loadings. (3) CPEV: cumulative percentage of explained variance (that of PCA loadings is denoted by CPEV(V)). (4) NOR: nonorthogonality of loadings, defined by $1/(r(r-1)) \sum_{i \neq j} |\cos \theta(X_i, X_j)|$ where r is the number of loadings. (5) Time cost. Sometimes we may use the worst sparsity among loadings, $\min_i(1 - \|X_i\|_0/p)$, instead of STD, when it is more appropriate to show the imbalance of sparsity among loadings.

6.1 Experimental Settings

All methods involved in the comparison have only one parameter λ controlling sparsity. For those methods that have direct control on sparsity, we also view them as belonging to T-sp and let λ be the prescribed number of zeros of a vector. GPowerB is initialized with PCA, and its parameters are set as $\mu_j = 1$, $\forall j$ and λ 's are uniform for all loadings.³ For ALSPCA, since we do not consider correlation among principal components, we set $\Delta_{ij} = +\infty$, $\epsilon_I = +\infty$, $\epsilon_E = 0.03$, and $\epsilon_O = 0.1$. In SPCArt, for T- ℓ_0 and T- ℓ_1 we set $\lambda = 1/\sqrt{p}$ by default, since it is the minimal threshold to ensure sparsity and the maximal threshold to avoid truncating to zero vector.

Termination conditions of SPCArt, SPCA are the relative change of loadings $\|X^{(t)} - X^{(t-1)}\|_F/\sqrt{r} < 0.01$ or iterations exceed 200. rSVD-GP(B) uses the same setting. All codes are implemented using MATLAB, run on a common desktop computer with the CPU of 2.93GHz duo core and 2GB memory. Except SPCArt and rSVD-GP, the others are downloaded from the authors' websites.

³The original random initialization for r-1 vectors [8] may fall out of data subspace and result in zero solution. When using PCA as initialization, distinct μ_j setting in effect artificially alters data variance.

Table 2: Recovering of sparse loadings on a synthetic data. $r = 2$. $\text{CPEV}(V) = 0.9973$. Loading pattern 5-10; 1-4,9-10 means the nonzero support of the first loading vector is 5 to 10, and the second is 1 to 4 and 9 to 10.

algorithm		λ	loading pattern	CPEV
SPCA	T-sp	4	5-10; 1-4	0.9848
	T- ℓ_1	2.2	1-4,9-10; 5-8	0.8286
PathSPCA	T-sp	4	5-10; 1-4,9-10	0.9960
ALSPCA		0.7	5-10; 1-4	0.9849
rSVD-GP	T- ℓ_0	$1/\sqrt{p}$	5-10; 1-4	0.9849
	T- ℓ_1	$1/\sqrt{p}$	5-10; 1-4	0.9808
	T-sp	4	5-10; 1-4,9-10	0.9960
	T-en	0.1	5-10; 1-4	0.9849
SPCArt	T- ℓ_0	$1/\sqrt{p}$	5-10; 1-4	0.9848
	T- ℓ_1	$1/\sqrt{p}$	5-10; 1-4	0.9728
	T-sp	4	5-10; 1-4,9-10	0.9968
	T-en	0.1	5-10; 1-4	0.9848

6.2 Synthetic Data

We will test whether SPCArt and rSVD-GP can recover some underlying sparse loadings. The synthetic data has been used by [6], considering three hidden Gaussian factors: $H_1 \sim N(0, 290)$, $H_2 \sim N(0, 300)$, $H_3 = -0.3H_1 + 0.925H_2 + \epsilon$, $\epsilon \sim N(0, 1)$, where H_1 , H_2 , and ϵ are independent. Then ten variables are generated: $A_i = H_j + \epsilon_i$, $\epsilon_i \sim N(0, 1)$, $i = 1, \dots, 10$, with $j = 1$ for $i = 1, \dots, 4$, $j = 2$ for $i = 5, \dots, 8$, $j = 3$ for $i = 9, 10$. In words, H_1 and H_2 are mutually independent random variables, while H_3 has correlations with both of them, in particular more with H_2 . The first 1-4 dimensions of data are mainly generated by the common factor H_1 ; while the 5-8 dimensions are mainly generated by H_2 ; so these two sets of dimensions are mutually independent; the last dimensions 9-10 are generated by H_3 , so they have correlations with both of the 1-4 and 5-8 dimensions with more with the latter. The covariance matrix C determined by A_i is fed into the algorithms. For those algorithms that only accept data matrix, an artificial data matrix $\tilde{A} = V\Sigma^{-1/2}V^T$ is made where $V\Sigma V^T = C$ is the SVD of C . This is reasonable since they share the same loadings.

The algorithms are tested to find two sparse loadings. Besides CPEV, the nonzero supports of the loadings are recorded, which should be consistent with the above generating model. We mainly focus on whether rSVD-GP and SPCArt can recover the underlying sparse patterns. The results are reported in Table 2. Except SPCA(T- ℓ_1), the others recover the more acceptable loading patterns, as can be seen from the CPEV.⁴

6.3 Pitprops Data

The Pitprops data is a classical data to test sparse PCA [23]. There is a covariance matrix of 13 variables available: $C \in \mathbb{R}^{13 \times 13}$. For those algorithms that only accept data matrix as input, an artificial data matrix $A = V\Sigma^{-1/2}V^T$ is made where $V\Sigma V^T = C$. The algorithms are tested to find $r = 6$ sparse loadings. For fairness, λ 's are tuned so that each algorithm yields total cardinality of all loadings, denoted by NZ, about 18; and mainly T-sp and T- ℓ_0 algorithms are tested. Criteria STD, NOR, and CPEV are reported. The results are shown in Table 3. For T- ℓ_0 , SPCArt does best overall, although its CPEV is not the best; the others, especially GPower(B), suffer from unbalanced cardinalities, as can be seen from the loading patterns and STD; their CPEV may be high but they are mainly contributed by the dense leading vector, which aligns with the direction of maximal variance, i.e. leading PCA loading. The improvements of rSVD-GP(B) over GPower(B) on this point is significant, as can be seen from the tradeoff between STD and CPEV. For T-sp, focusing on NOR and CPEV, the performance of rSVD-GP is good while that of SPCArt is somewhat bad in this case, for the CPEV is the worst although the NOR ranks two.

⁴Setting $\lambda = 6$ for T-sp, all recover another well accepted 5-8; 1-4 pattern, see [13] for detail.

Table 3: A comparison of algorithms on the Pitprops data. $r = 6$, $\text{CPEV}(V) = 0.8700$. Loading patterns here describe the cardinality of each loading vector.

algorithm	λ	NZ	loading patterns	STD	NOR	CPEV	
ALSPCA	0.65	17	722213	0.1644	0.0008	0.8011	
T- ℓ_0	GPower	0.1	19	712162	0.2030	0.0259	0.8111
	rSVD-GP	0.27	17	612422	0.1411	0.0209	0.8117
	GPowerB	0.115	17	724112	0.1782	0.0186	0.8087
	rSVD-GPB	0.3	18	534132	0.1088	0.0222	0.7744
	SPCArt	$1/\sqrt{p}$	18	424332	0.0688	0.0181	0.8013
T-sp	SPCA	10	18	333333	0	0.0095	0.7727
	PathSPCA	10	18	333333	0	0.0484	0.7840
	rSVD-GP	10	18	333333	0	0.0455	0.7819
	rSVD-GPB	10	18	333333	0	0.0525	0.7610
	SPCArt	10	18	333333	0	0.0428	0.7514

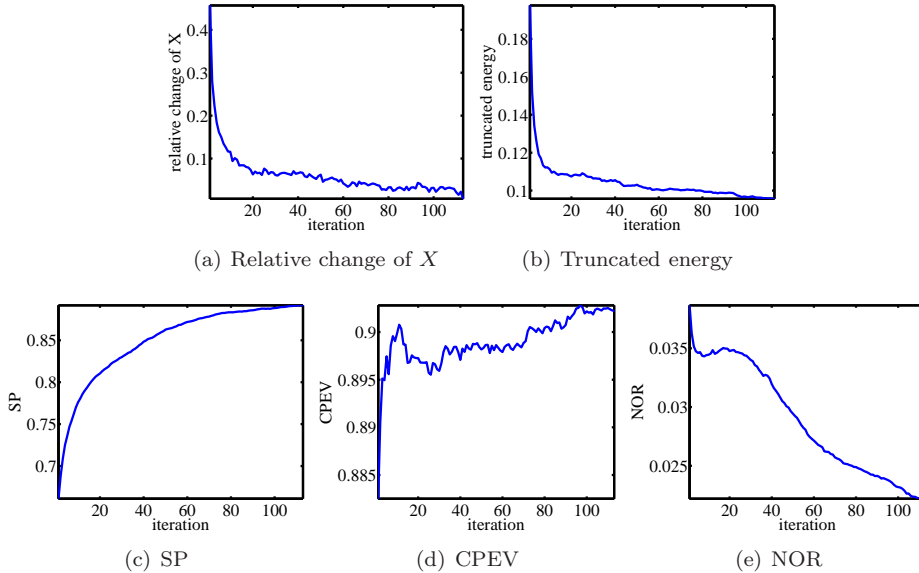


Figure 1: Convergence of SPCArt(T- ℓ_0) on image data. The convergence is relatively stable, and the criteria improve along with the iteration.

6.4 Natural Image Data

The investigation of distribution of natural image patches is important for computer vision and pattern recognition communities. On this data set, we will evaluate the convergence and performance bounds of SPCArt, and make a comprehensive comparisons between different algorithms over a range of sparsity and r . We randomly select 5000 gray-scale 13×13 patches from BSDS [26]. Each patch is reshaped to a vector of dimension 169. The DC component of each patch is removed first, and then the mean of data set is removed.

6.4.1 Convergence of SPCArt

We will show the stability of convergence and improvement of SPCArt over simple thresholding [5]. We take T- ℓ_0 ($\lambda = 1/\sqrt{p}$) as example. $r = 70$, $\text{CPEV}(V) = 0.95$. The results are shown in Figure 1. Gradually, SPCArt has found a local optimal rotation such that less truncated energy from the rotated PCA loadings is needed (Figure 1(b)) to get a sparser (Figure 1(c)), more variance explained (Figure 1(d)), and more orthogonal (Figure 1(e)) basis. Note that, the results in the first iteration are equal to those

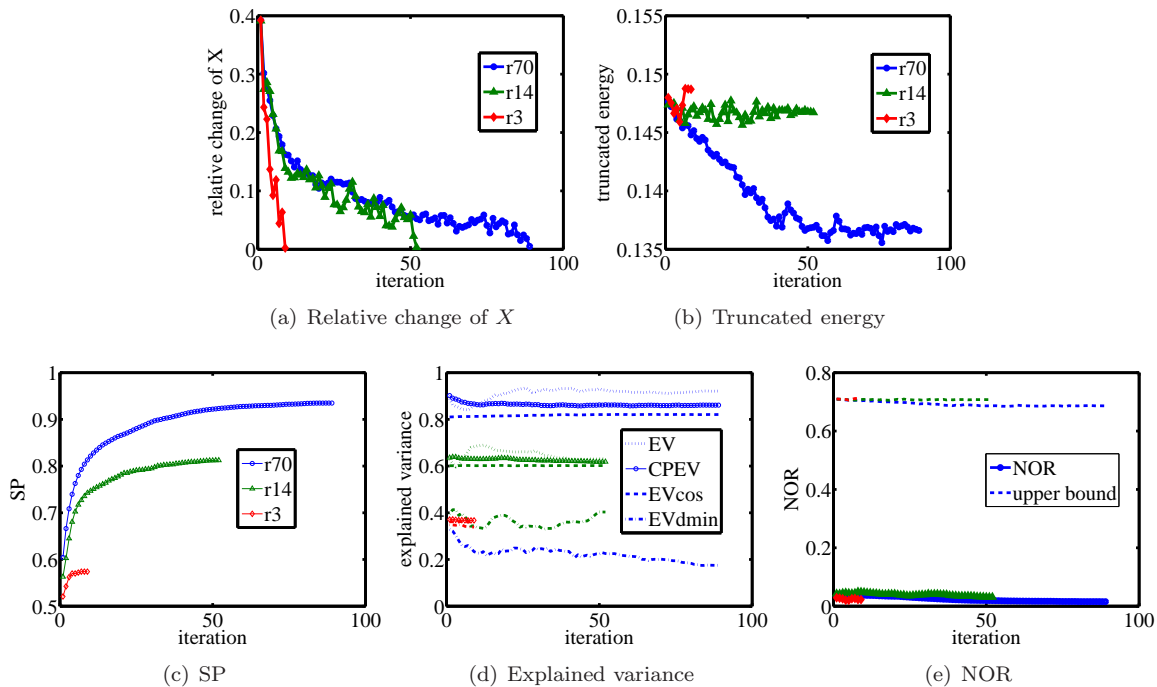


Figure 2: Performance bounds of SPCArt(T-en) for 3 levels of r on image data. In (d), EV is a normalized version $EV = \text{tr}(X^T A^T A X) / \text{tr}(A^T A)$ so that it can be compared with CPEV. $EV_{\text{dmin}} = d_{\text{min}}^2 EV(V) / \text{tr}(A^T A)$ and $EV_{\text{cos}} = \cos^2(\theta) EV(V) / \text{tr}(A^T A)$. We see EV_{cos} is better than EV_{dmin} in estimation, and EV_{cos} meets empirical performance well. For NOR, the algorithm performs far optimistic than those upper bounds. Owing to the good orthogonality, EV are comparable to CPEV. For each r , as iteration goes, SP improves a lot while CPEV sacrifices little. As r increases, all criteria improve.

of simple thresholding [5]. It is evident that SPCArt significantly improves over simple thresholding.

6.4.2 Performance Bounds of SPCArt

We now compare the theoretical bounds provided in Section 3.3 with empirical performance. T-en with $\lambda = 0.15$ is taken as example, so that about 85% EV(V) is guaranteed. To achieve a more systematic evaluation, three levels of subspace dimension are tested: $r = [3 \ 14 \ 70]$ with the corresponding CPEV(V) = [0.42 0.71 0.95]. The results are shown in Figure 2. Note that most of the theoretical bounds are absolute bounds without assuming specific distribution of data, so they may be very different from empirical performance.

First, for sparsity, the lower bound given in (18) is about 15%. But as seen in Figure 2(c), empirical sparsity is far better than expectation, especially when r is larger.

Similar situation occurs for nonorthogonality, as seen in Figure 2(e). The upper bounds are far too pessimistic to be practical. It may be caused by the high dimension 169 of data.

Finally, for explained variance, it can be found from Figure 2(d) that there is no large discrepancy between EV and CPEV, owing to the near orthogonality of the sparse basis as indicated in Figure 2(e). On the other hand, the specific bound EV_{cos} is better than the universal bound EV_{dmin} . In contrast to sparsity and nonorthogonality, EV_{cos} meets the empirical performance well, as analyzed in Section 3.3.

6.4.3 Performance Comparisons between Algorithms Based on SP

We fix $r = 70$ and run the algorithms over a range of parameter λ to produce a series of results, then the other criteria are plotted against SP. We will first verify two points: the improvement of rSVD-GP over GPower(B) on the balance of sparsity is significant, and take rSVD-GP(B) as example to show that

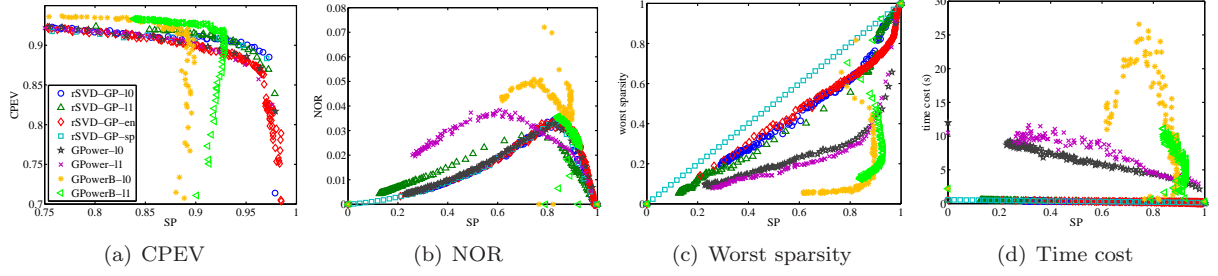


Figure 3: rSVD-GP v.s. GPower(B) on image data. From (c), we see for GPower(B), the uniform parameter setting leads to unbalanced sparsity, the worst case is rather dense. rSVD-GP significantly improves over GPower(B) on balance of sparsity as well as other criteria.

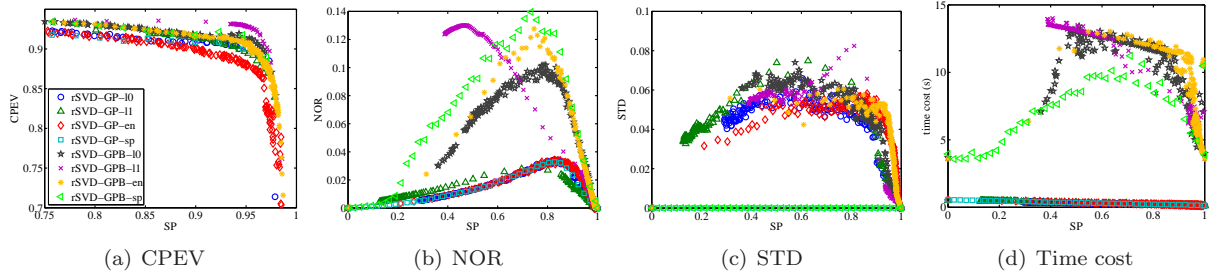


Figure 4: rSVD-GP v.s. rSVD-GPB on image data. Both are initialized with PCA. From (b), we see the block version gets much worse orthogonality than the deflation version. The other criteria are comparable except time cost.

block algorithm produces worse orthogonality than deflation algorithm. Then we compare SPCArt with the other algorithms.

(1) rSVD-GP v.s. GPower(B), see Figure 3. For GPower(B), uniform parameter setting leads to unbalanced sparsity. In fact, the worst case is usually achieved by the leading ones. rSVD-GP significantly improves over GPower(B) on this criterion as well as the others.

(2) rSVD-GP v.s. rSVD-GPB, see Figure 4. The block case always gets worse orthogonality. This is because there is no mechanism in it to ensure orthogonality.

(3) SPCArt v.s. rSVD-GP, see Figure 5. The two methods obtain comparable results over these criteria.

(4) SPCArt v.s. SPCA, PathSPCA, and ALSPCA, see Figure 6. SPCArt performs best overall. Generally, PathSPCA performs best at CPEV, but its time cost increases with cardinality. ALSPCA is unstable and sensitive to parameter, so is SPCA. Besides, SPCA is time consuming.

6.4.4 Performance Comparisons between Algorithms Based on r

Finally, with fixed λ , we evaluate how performance changes as r increases. r is sampled so that $\text{CPEV}(V) = [0.3 \ 0.5 \ 0.7 \ 0.8 \ 0.9 \ 0.95 \ 0.99 \ 1]$. λ 's are set as follows. T- ℓ_0 : $1/\sqrt{p}$; T-sp: $[0.85p]$; T-en: 0.15; T- ℓ_1 : SPCArt $1/\sqrt{p}$, SPCA 4, ALSPCA 0.7. The results are plotted in Figure 7, in which it can be found that:

(1) Using the same threshold, T- ℓ_1 is always more sparse and orthogonal than T- ℓ_0 , while explaining less variance.

(2) SPCArt is insensitive to parameter. A constant setting produces satisfactory results across r 's. But it is not the case for rSVD-GP.

(3) In contrast to deflation algorithms (PathSPCA, rSVD-GP), SPCArt is a block algorithm, which computes r loadings together. So the obtained loadings tend to be more globally optimal. This is evident for T-en and T- ℓ_1 when r becomes the full dimension 169. T- ℓ_1 perfectly recovers the natural basis which is globally optimal; and T-en obtains similar results. Visualized images of the loadings of the deflation

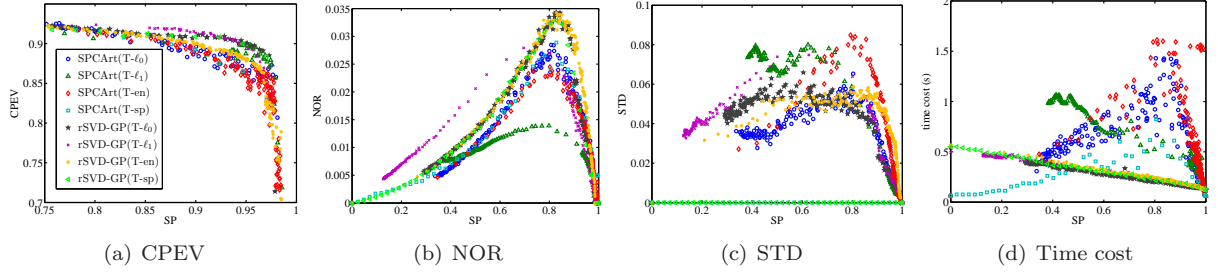


Figure 5: SPCArt v.s. rSVD-GP on image data. The two methods obtain comparable results over these criteria.

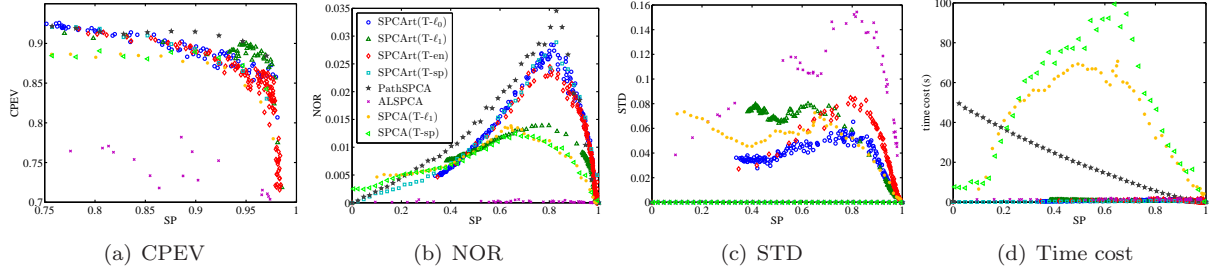


Figure 6: SPCArt v.s. SPCA, PathSPCA, ALSPCA on image data. SPCArt performs best overall, while PathSPCA performs best at CPEV. ALSPCA and SPCA are unstable. PathSPCA and SPCA are time consuming.

and block algorithm are shown in Figure 8. Due to the greedy nature, the results obtained by deflation algorithm are more confined to those of PCA; and the first 10 loadings differ significantly from the last 10 loadings.

6.5 Gene Data ($n \ll p$)

We now try the algorithms on a Leukemia dataset [24], which contains 7129 genes and 72 samples, i.e. $p \gg n$ data. This is a classical application that motivates the development of sparse PCA. Because from the thousands of genes, a sparse basis can help us to locate a few of them that determines the distribution of data. The results are shown in Figure 9. For this type of data, SPCA is run on the $p \gg n$ mode [6] for efficiency. PathSPCA is very slow except when $SP \geq 97\%$, so it is not involved in the comparison. The mean iterations and time cost are reported as follows: SPCArt($T-l_0$), ($T-l_1$), ($T-en$), ($T-sp$) are (94, 0.67), (12, 0.38), (83, 0.80), (73, 0.74) respectively; rSVD-GP($T-l_0$) (11, 0.42); ALSPCA (8, 8.89); SPCA($T-l_1$) (8, 0.41). SPCArt($T-l_0$) and rSVD-GP($T-l_0$) perform best (the later is slightly better).

6.6 Random Data ($n > p$)

Finally, we test the computational efficiency on a set of random data with increasing dimensions $p = [100 \ 400 \ 700 \ 1000 \ 1300]$. Following GPower [8], zero-mean, unit-variance Gaussian data is used for the test. To make how the computational cost depends on p clear, we let $n = p + 1$. For fair comparison, only T-sp with $\lambda = \lfloor 0.85p \rfloor$ are tested. r is set to 20. The results are shown in Figure 10. rSVD-GP and PathSPCA increase nonlinearly against p , while SPCArt grows much slowly. Remember in previous Figure 6(d), we already showed that the time complexity of PathSPCA increases nonlinearly against the cardinality, and from Figure 7(f), we saw SPCArt increases nonlinearly against r . All these are consistent with Table 1. When dealing with high dimensional data and pursuing a few loadings, SPCArt has more advantages.

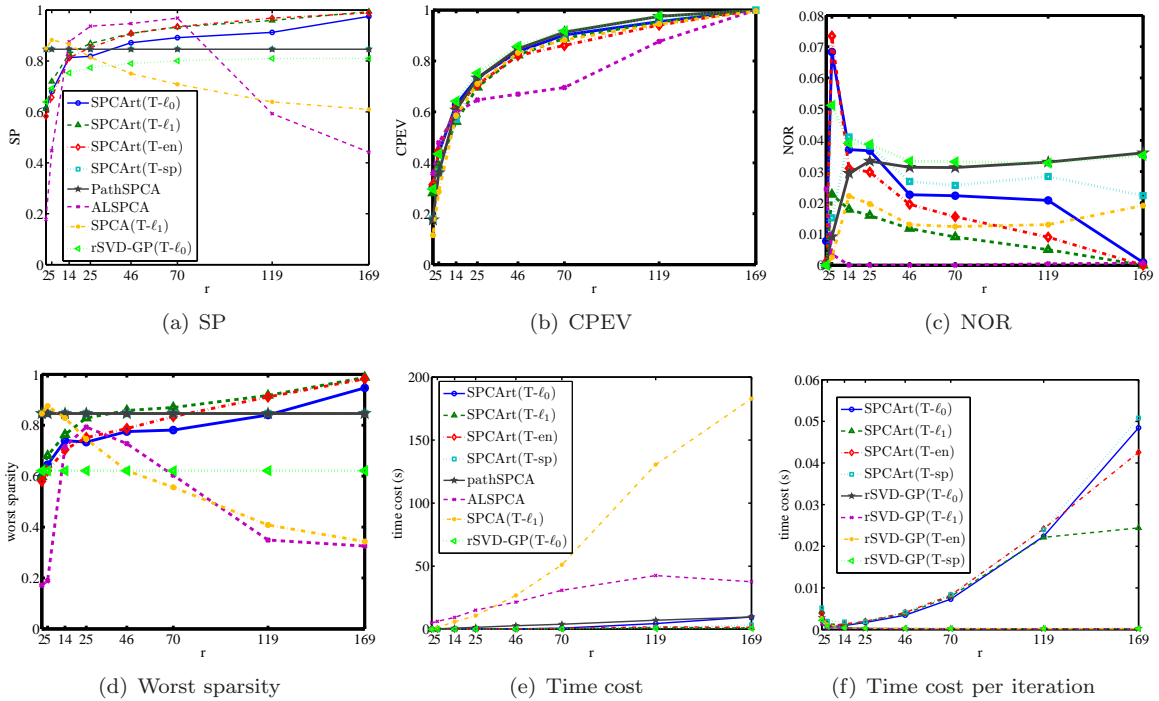


Figure 7: Performance under a range of r on image data, SPCArt v.s. SPCA, PathSPCA, ALSPCA, and rSVD-GP(T- ℓ_0). In (f), only SPCArt and rSVD-GP are shown. SPCArt is insensitive to parameter setting and the loadings are adaptive with r . When r becomes the full dimension of 169, T- ℓ_1 perfectly recovers the natural basis which is globally optimal, as can be seen from SP, worst sparsity, and NOR. Both the two sparsity criteria reach $(p-1)/p = 0.994$ and NOR touches bottom 0. T-en achieves similar results.

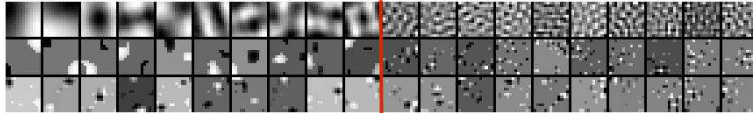


Figure 8: Images of the first 10 and last 10 loadings among total 70 on image data. 1st line: PCA; 2nd line: rSVD-GP(T-sp); 3rd line: SPCArt(T-sp). $\lambda = \lfloor 0.85p \rfloor$. rSVD-GP is greedy, and the results of it are more confined to those of PCA, while SPCArt is more flexible.

7 Conclusion

We have proposed a new sparse PCA model, called SPCArt, with performance analysis provided; and we have extended GPower and rSVD to an improved version, called rSVD-GP. Performance comparisons between our methods and various existing methods were conducted. According to the experiments, SPCArt and rSVD-GP generally outperformed the others. They obtained a good trade-off between sparsity, explained variance, orthogonality, and balance of sparsity. Compared with SPCArt, rSVD-GP is more sensitive to parameter setting (except rSVD-GP(T-sp), i.e. TPower) and the solution obtained is less globally optimal. SPCArt is capable of dealing with high dimensional, large sample-size data so long as the target sparse loadings are not too many.

The four truncation types of SPCArt work well in different aspects: T- ℓ_0 hard thresholding performs well overall; T- ℓ_1 soft thresholding gets best sparsity and orthogonality; T-sp hard sparsity constraint directly controls sparsity and has zero sparsity variance; T-en truncation by energy percentage guarantees explained variance.

As for future work, we would research the following problems: (1) under what conditions can SPCArt,

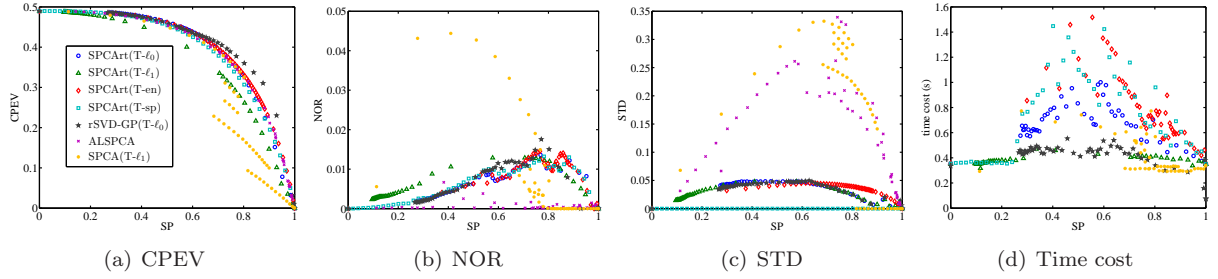


Figure 9: SPCArt vs. rSVD-GP($T-\ell_0$), ALSPCA, SPCA($T-\ell_1$) on gene data, $r = 6$. ALSPCA is much more costly so it is not shown in (d). SPCArt($T-\ell_0$) and rSVD-GP($T-\ell_0$) perform best, and both are able to finish within 1 second in such high dimensional data.

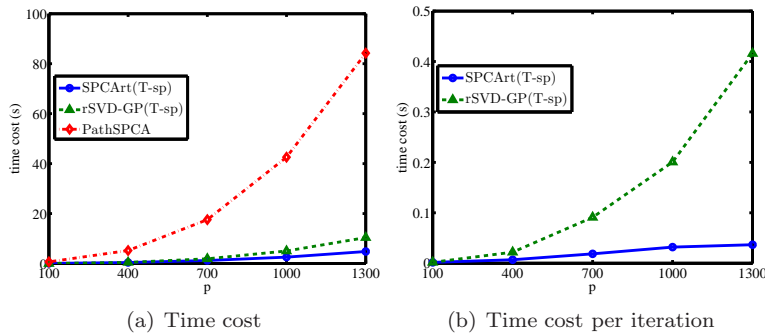


Figure 10: Speed test on random data with increasing dimension p . SPCArt grows much slowly as p .

with each truncation type, recover the underlying sparse basis? Efforts have been made recently on this problem [27, 28, 9, 21]; (2) is there any explicit objective formulation for the T-en?

A Proofs of Performance Bounds of SPCArt

Many of the results can be proven by studying the special case $z = (1, 0, \dots, 0)^T$ and $z = (1/\sqrt{p}, \dots, 1/\sqrt{p})^T$. We mainly focus on the less straightforward ones.

A.1 Sparsity and Deviation

Proposition 7. For $T-\ell_0$ (13), the sparsity bounds are

$$\begin{cases} 0 \leq s(x) \leq 1 - \frac{1}{p} & , \lambda < \frac{1}{\sqrt{p}}, \\ 1 - \frac{1}{p\lambda^2} \leq s(x) \leq 1 & , \lambda \geq \frac{1}{\sqrt{p}}. \end{cases}$$

Deviation $\sin(\theta(x, z)) = \|\bar{z}\|_2$, where \bar{z} is the truncated part: $\bar{z}_i = z_i$ if $x_i = 0$, and $\bar{z}_i = 0$ otherwise. The absolute bounds are:

$$0 \leq \sin(\theta(x, z)) \leq \begin{cases} \sqrt{p-1}\lambda & , \lambda < \frac{1}{\sqrt{p}}, \\ 1 & , \lambda \geq \frac{1}{\sqrt{p}}. \end{cases}$$

All the above bounds are achievable.

Proof. We only prove $1 - \frac{1}{p\lambda^2} \leq s(x)$, if $\lambda \geq \frac{1}{\sqrt{p}}$. The others are easy to obtain. Let $\tilde{z} = z - \bar{z}$, i.e. the part above λ , and let $k = \|\tilde{z}\|_0$, then $k\lambda^2 < \|\tilde{z}\|_2^2 \leq 1$. So $k < 1/\lambda^2$. Since $\|x\|_0 = \|\tilde{z}\|_0$, $s(x) = 1 - \|x\|_0/p > 1 - 1/(p\lambda^2)$. \square

Proposition 8. For $T\text{-}\ell_1$ (11), the bounds of $s(x)$ and lower bound of $\sin(\theta(x, z))$ are the same as $T\text{-}\ell_0$. In addition, there are relative deviation bounds

$$\|\bar{z}\|_2 \leq \sin(\theta(x, z)) < \sqrt{\|\bar{z}\|_2^2 + \lambda^2 \|x\|_0}.$$

Proof. Let $\tilde{z} = z - \bar{z}$, $\hat{z} = S_\lambda(z)$ and $y = \tilde{z} - \hat{z}$. Note that the absolute value of nonzero entry of y is λ , and $\|y\|_2 = \lambda\sqrt{\|\tilde{z}\|_0} = \lambda\sqrt{\|x\|_0}$. Then,

$$\cos(\theta(x, z)) = \cos(\theta(\hat{z}, z)) = \hat{z}^T z / \|\hat{z}\|_2. \quad (31)$$

Expand $z = \hat{z} + y + \bar{z}$ and note that \bar{z} is orthogonal to \tilde{z} and \hat{z} , since their support do not overlap. We have,

$$\hat{z}^T z = \|\hat{z}\|_2^2 + \hat{z}^T y. \quad (32)$$

By the soft thresholding operation,

$$0 < \hat{z}^T y \leq \|\hat{z}\|_2 \|y\|_2. \quad (33)$$

Combining (31), (32) and (33), we have $\|\hat{z}\|_2 < \cos(\theta(x, z)) \leq \|\hat{z}\|_2 + \|y\|_2$. Note that the upper bound of (33) is achieved when \hat{z} and y are in the same direction, and in this case, $\|\hat{z}\|_2 + \|y\|_2 = \|\tilde{z}\|_2$. So $\|\hat{z}\|_2 < \cos(\theta(x, z)) \leq \|\tilde{z}\|_2$. Then $1 - \|\tilde{z}\|_2^2 \leq \sin^2(\theta(x, z)) < 1 - \|\hat{z}\|_2^2$. The upper bound is approached when \hat{z} becomes orthogonal to y , in this case $\|\hat{z}\|_2^2 + \|y\|_2^2 + \|\bar{z}\|_2^2 = \|z\|_2^2 = 1$. Hence, $1 - \|\hat{z}\|_2^2 = \|\bar{z}\|_2^2 + \|y\|_2^2 = \|\bar{z}\|_2^2 + \lambda^2 \|x\|_0$. Besides, $1 - \|\tilde{z}\|_2^2 = \|\bar{z}\|_2^2$. The final result is $\|\bar{z}\|_2 \leq \sin(\theta(x, z)) < \sqrt{\|\bar{z}\|_2^2 + \lambda^2 \|x\|_0}$. \square

Proposition 10. For $T\text{-en}$, $0 \leq \sin(\theta(x, z)) \leq \sqrt{\lambda}$. Usually, $\sin(\theta(x, z)) \approx \sqrt{\lambda}$. In addition

$$\lfloor \lambda p \rfloor / p \leq s(x) \leq 1 - 1/p.$$

If $\lambda < 1/p$, there is no sparsity guarantee. When p is moderately large, $\lfloor \lambda p \rfloor / p \approx \lambda$.

Proof. Sort squared elements of z in ascending order, and assume they are $\hat{z}_1^2 \leq \hat{z}_2^2 \leq \dots \leq \hat{z}_p^2$ and the first k of them are truncated. If z is uniform, i.e. $\hat{z}_1^2 = \hat{z}_p^2 = 1/p$, then the number of truncated entries is $k_0 = \lfloor \lambda p \rfloor$. Suppose $\exists z$ achieves $k < k_0$, then $\sum_{i=1}^{k_0} \hat{z}_i^2$ is greater than that of uniform case i.e. $\sum_{i=1}^{k_0} \hat{z}_i^2 > k_0/p$. By the ordering, $\hat{z}_{k_0}^2$ is above the mean of the first k_0 entries, $\hat{z}_{k_0}^2 \geq 1/k_0 \sum_{i=1}^{k_0} \hat{z}_i^2 > 1/p$. But on the other hand, $\hat{z}_{k_0+1}^2$ is below the mean of the remaining part, $\hat{z}_{k_0+1}^2 \leq 1/(p - k_0) \sum_{i=k_0+1}^p \hat{z}_i^2 < 1/(p - k_0)(1 - k_0/p) = 1/p < \hat{z}_{k_0}^2$, i.e. $\hat{z}_{k_0+1}^2 < \hat{z}_{k_0}^2$ which is a contradiction. Thus, $\lfloor \lambda p \rfloor / p \leq s(x)$. \square

Proposition 11 can be proved in a way similar to $T\text{-en}$.

A.2 Explained Variance

Theorem 12. Let rank r SVD of $A \in \mathbb{R}^{n \times p}$ be $U\Sigma V^T$, $\Sigma \in \mathbb{R}^{r \times r}$. Given $X \in \mathbb{R}^{p \times r}$, assume SVD of $X^T V$ is $W D Q^T$, $D \in \mathbb{R}^{r \times r}$, $d_{\min} = \min_i D_{ii}$. Then

$$d_{\min}^2 \cdot EV(V) \leq EV(X),$$

and $EV(V) = \sum_i \Sigma_{ii}^2$.

Proof. Let SVD of $A^T A$ be $[V, V_2] \begin{bmatrix} \Lambda & \\ & \Lambda_2 \end{bmatrix} \begin{bmatrix} V^T \\ V_2^T \end{bmatrix}$, where $\Lambda = \Sigma^2$ and subscript 2 associates with the remaining loadings. Then

$$\begin{aligned} \text{tr}(X^T A^T A X) &= \text{tr}(X^T [V, V_2] \begin{bmatrix} \Lambda & \\ & \Lambda_2 \end{bmatrix} \begin{bmatrix} V^T \\ V_2^T \end{bmatrix} X) \\ &= \text{tr}(X^T V \Lambda V^T X) + \text{tr}(X^T V_2 \Lambda_2 V_2^T X) \\ &\geq \text{tr}(X^T V \Lambda V^T X) \\ &= \text{tr}(W D Q^T \Lambda Q D W^T) \\ &= \text{tr}(Q^T \Lambda Q D^2) \\ &\geq \text{tr}(Q^T \Lambda Q) d_{\min}^2 \\ &= d_{\min}^2 \sum_i \Lambda_{ii}. \end{aligned}$$

□

Theorem 13. Let $C = Z^T X$, i.e. $C_{ij} = \cos(\theta(Z_i, X_j))$, and let \bar{C} be C with diagonal elements removed. Assume $\theta(Z_i, X_i) = \theta$ and $\sum_j C_{ij}^2 \leq 1, \forall i$, then

$$(\cos^2(\theta) - \sqrt{r-1} \sin(2\theta)) \cdot EV(V) \leq EV(X).$$

When θ is sufficiently small,

$$(\cos^2(\theta) - O(\theta)) \cdot EV(V) \leq EV(X).$$

Proof. Following the notations of the previous theorem,

$$\begin{aligned} & tr(X^T A^T A X) \\ & \geq tr(X^T V \Lambda V^T X) \\ & = tr(X^T V R^T R \Lambda R^T R V^T X) \\ & = tr(C^T R \Lambda R^T C) \\ & = tr(R \Lambda R^T C C^T) \\ & = tr(R \Lambda R^T (I \cos(\theta) + \bar{C})(I \cos(\theta) + \bar{C}^T)) \\ & = tr(R \Lambda R^T (I \cos^2(\theta) + (\bar{C} + \bar{C}^T) \cos(\theta) + \bar{C} \bar{C}^T)) \\ & \geq tr(\Lambda) \cos^2(\theta) + tr(R \Lambda R^T (\bar{C} + \bar{C}^T)) \cos(\theta). \end{aligned}$$

We estimate the minimum eigenvalue λ_{min} of the symmetric matrix $S = \bar{C} + \bar{C}^T$. By Gershgorin circle theorem, $|\lambda_{min}| \leq \sum_{j \neq i}^r |S_{ij}|, \forall i$, since $S_{ii} = 0$.

$$\begin{aligned} \sum_{j \neq i}^r |S_{ij}| &= \sum_{j \neq i}^r |\cos(\theta(Z_i, X_j)) + \cos(\theta(X_i, Z_j))| \\ &\leq \sum_{j \neq i}^r |\cos(\theta(Z_i, X_j))| + \sum_{j \neq i}^r |\cos(\theta(X_i, Z_j))| \\ &\leq \sqrt{r-1} \left(\sum_{j \neq i}^r |\cos(\theta(Z_i, X_j))|^2 \right)^{-1/2} \\ &\quad + \sqrt{r-1} \left(\sum_{j \neq i}^r |\cos(\theta(X_i, Z_j))|^2 \right)^{-1/2}. \end{aligned}$$

The last inequality holds since, $\forall x \in \mathbb{R}^p, \|x\|_1 \leq \sqrt{p} \|x\|_2$. Because Z is the r orthonormal vectors, $\|Z^T X_i\|_2 \leq \|X_i\|_2 = 1$, and $Z_j^T X_i = \cos(\theta(X_i, Z_j))$, hence $\sum_{j \neq i}^r |\cos(\theta(X_i, Z_j))|^2 \leq 1 - \cos^2(\theta) = \sin^2(\theta)$. And by assumption, $\sum_j C_{ij}^2 \leq 1$, so we also have $\sum_{j \neq i}^r |\cos(\theta(Z_i, X_j))|^2 \leq \sin^2(\theta)$. Thus, $\sum_{j \neq i}^r |S_{ij}| \leq 2\sqrt{r-1} \sin(\theta)$, and $\lambda_{min} \geq -2\sqrt{r-1} \sin(\theta)$. Finally,

$$\begin{aligned} tr(X^T A^T A X) &\geq tr(\Lambda) \cos^2(\theta) + tr(R \Lambda R^T (\bar{C} + \bar{C}^T)) \cos(\theta) \\ &\geq EV(V) \cos^2(\theta) + EV(V) \lambda_{min} \cos(\theta) \\ &= (\cos^2(\theta) - 2\sqrt{r-1} \cos(\theta) \sin(\theta)) EV(V) \\ &= (\cos^2(\theta) - \sqrt{r-1} \sin(2\theta)) EV(V). \end{aligned}$$

When θ is sufficiently small, such that $\sin(2\theta) \approx 2\theta$, we have $tr(X^T A^T A X) \geq (\cos^2(\theta) - O(\theta)) EV(V)$. □

B Deducing Original GPower from Matrix Approximation Formulation

First, we give the original GPower. Fixing Y , (26) and (27) have solutions $W_i^* = H_{\sqrt{\lambda_i}}(A^T Y_i) / \|H_{\sqrt{\lambda_i}}(A^T Y_i)\|_2$ and $W_i^* = S_{\lambda_i}(A^T Y_i) / \|S_{\lambda_i}(A^T Y_i)\|_2$ respectively. Substituting them into original objectives, the ℓ_0 problem becomes

$$\max_Y \sum_i \sum_j [(A_j^T Y_i)^2 - \lambda_i]_+, \quad s.t. Y^T Y = I, \quad (34)$$

and the ℓ_1 problem becomes $\max_Y \sum_i \sum_j [|A_j^T Y_i| - \lambda_i]_+, \quad s.t. Y^T Y = I$. Actually, it is to solve

$$\max_Y \sum_i \sum_j [|A_j^T Y_i| - \lambda_i]_+^2, \quad s.t. Y^T Y = I. \quad (35)$$

Now the problem is to maximize two convex functions, [8] approximately solves them via a gradient method which is generalized power method. The t th iteration is provided by

$$Y^{(t)} = \text{Polar}(A H_{\sqrt{\lambda_i}}(A^T Y^{(t-1)})), \quad (36)$$

and

$$Y^{(t)} = \text{Polar}(A S_{\lambda_i}(A^T Y^{(t-1)})). \quad (37)$$

We now see how these can be deduced from the matrix approximation formulations (28) and (29). Split X into $X = WD$, $s.t. \|W_i\|_2 = 1, \forall i$ and $D > 0$ is diagonal matrix whose diagonal element d_i in fact models the length of the corresponding column of X . Then they become

$$\begin{aligned} \min_{Y,D,W} & \|A - YDW^T\|_F^2 + \sum_i \lambda_i \|W_i\|_0, \\ & = \|A\|_F^2 + \sum_i d_i^2 - 2 \sum_i d_i Y_i^T A W_i + \sum_i \lambda_i \|W_i\|_0, \\ & \quad s.t. Y^T Y = I, D > 0 \text{ is diagonal}, \|W_i\|_2 = 1, \forall i, \end{aligned} \quad (38)$$

and

$$\begin{aligned} \min_{Y,D,W} & \frac{1}{2} \|A - YDW^T\|_F^2 + \sum_i \lambda_i \|d_i W_i\|_1, \\ & = \frac{1}{2} \|A\|_F^2 + \frac{1}{2} \sum_i d_i^2 - \sum_i d_i Y_i^T A W_i + \sum_i \lambda_i d_i \|W_i\|_1, \\ & \quad s.t. Y^T Y = I, D > 0 \text{ is diagonal}, \|W_i\|_2 = 1, \forall i. \end{aligned} \quad (39)$$

Fix Y and W , and solve D . For the ℓ_0 case, $d_i^* = Y_i^T A W_i$. Substituting it back, we get (26).

For the ℓ_1 case, $d_i^* = Y_i^T A W_i - \lambda_i \|W_i\|_1$. Assume λ_i is sufficiently small, then $d_i > 0$ is satisfied. Substituting it back we get $\max_{Y,W} \sum_i (Y_i^T A W_i - \lambda_i \|W_i\|_1)^2, \quad s.t. Y^T Y = I, \forall i, \|W_i\|_2 = 1$. When we fix Y and solve W , under the previous assumption it is equivalent to (27). Substituting $W_i^* = S_{\lambda_i}(A^T Y_i) / \|S_{\lambda_i}(A^T Y_i)\|_2$ back, we obtain (35).

Finally, we can see that the solutions (36) and (37) literally combine the two solution steps of (28) and (29) respectively.

Acknowledgment

This work was partly supported by National 973 Program (2013CB329500), National Natural Science Foundation of China (No. 61103107 and No. 61070067), and Research Fund for the Doctoral Program of Higher Education of China (No. 20110101120154).

References

- [1] I. Jolliffe, *Principal component analysis*. Springer-Verlag (New York), 1986.
- [2] A. d’Aspremont, F. Bach, and L. Ghaoui, “Optimal solutions for sparse principal component analysis,” *Journal of Machine Learning Research*, vol. 9, pp. 1269–1294, 2008.
- [3] I. Jolliffe, N. Trendafilov, and M. Uddin, “A modified principal component technique based on the lasso,” *Journal of Computational and Graphical Statistics*, vol. 12, no. 3, pp. 531–547, 2003.
- [4] L. Mackey, “Deflation methods for sparse pca,” *Advances in Neural Information Processing Systems*, vol. 21, pp. 1017–1024, 2009.
- [5] J. Cadima and I. Jolliffe, “Loading and correlations in the interpretation of principle compenents,” *Journal of Applied Statistics*, vol. 22, no. 2, pp. 203–214, 1995.
- [6] H. Zou, T. Hastie, and R. Tibshirani, “Sparse principal component analysis,” *Journal of computational and graphical statistics*, vol. 15, no. 2, pp. 265–286, 2006.
- [7] Z. Lu and Y. Zhang, “An augmented lagrangian approach for sparse principal component analysis,” *Mathematical Programming*, pp. 1–45, 2009.
- [8] M. Journée, Y. Nesterov, P. Richtárik, and R. Sepulchre, “Generalized power method for sparse principal component analysis,” *Journal of Machine Learning Research*, vol. 11, pp. 517–553, 2010.
- [9] X. Yuan and T. Zhang, “Truncated power method for sparse eigenvalue problems,” *Journal of Machine Learning Research*, vol. 14, pp. 899–925, 2013.
- [10] I. Jolliffe, “Rotation of principal components: choice of normalization constraints,” *Journal of Applied Statistics*, vol. 22, no. 1, pp. 29–35, 1995.
- [11] R. Tibshirani, “Regression shrinkage and selection via the lasso,” *Journal of the Royal Statistical Society. Series B (Methodological)*, pp. 267–288, 1996.
- [12] H. Zou and T. Hastie, “Regularization and variable selection via the elastic net,” *Journal of the Royal Statistical Society: Series B (Statistical Methodology)*, vol. 67, no. 2, pp. 301–320, 2005.
- [13] H. Shen and J. Huang, “Sparse principal component analysis via regularized low rank matrix approximation,” *Journal of multivariate analysis*, vol. 99, no. 6, pp. 1015–1034, 2008.
- [14] D. Witten, R. Tibshirani, and T. Hastie, “A penalized matrix decomposition, with applications to sparse principal components and canonical correlation analysis,” *Biostatistics*, vol. 10, no. 3, p. 515, 2009.
- [15] A. d’Aspremont, L. El Ghaoui, M. Jordan, and G. Lanckriet, “A direct formulation for sparse pca using semidefinite programming,” *SIAM Review*, vol. 49, no. 3, pp. 434–448, 2007.
- [16] Y. Zhang and L. El Ghaoui, “Large-scale sparse principal component analysis with application to text data,” 2011.
- [17] B. Moghaddam, Y. Weiss, and S. Avidan, “Spectral bounds for sparse pca: Exact and greedy algorithms,” *Advances in Neural Information Processing Systems*, vol. 18, p. 915, 2006.
- [18] —, “Generalized spectral bounds for sparse lda,” in *Proceedings of the 23rd international conference on Machine learning*. ACM, 2006, pp. 641–648.
- [19] Y. Zhang, A. d’Aspremont, and L. Ghaoui, “Sparse pca: Convex relaxations, algorithms and applications,” *Handbook on Semidefinite, Conic and Polynomial Optimization*, pp. 915–940, 2012.
- [20] G. Golub and C. Van Loan, *Matrix computations*. Johns Hopkins Univ Pr, 1996, vol. 3.

- [21] Z. Ma, “Sparse principal component analysis and iterative thresholding,” *The Annals of Statistics*, vol. 41, no. 2, pp. 772–801, 2013.
- [22] C. Eckart and G. Young, “The approximation of one matrix by another of lower rank,” *Psychometrika*, vol. 1, no. 3, pp. 211–218, 1936.
- [23] J. Jeffers, “Two case studies in the application of principal component analysis,” *Applied Statistics*, pp. 225–236, 1967.
- [24] T. Golub, D. Slonim, P. Tamayo, C. Huard, M. Gaasenbeek, J. Mesirov, H. Coller, M. Loh, J. Downing, M. Caligiuri, *et al.*, “Molecular classification of cancer: class discovery and class prediction by gene expression monitoring,” *Science*, vol. 286, no. 5439, p. 531, 1999.
- [25] K. Sjöstrand, “Matlab implementation of lasso, lars, the elastic net and spca,” *Informatics and Mathematical Modelling, Technical University of Denmark (DTU)*, 2005.
- [26] D. Martin, C. Fowlkes, D. Tal, and J. Malik, “A database of human segmented natural images and its application to evaluating segmentation algorithms and measuring ecological statistics,” in *International Conference on Computer Vision*. IEEE, 2001, pp. 416–423.
- [27] A. Amini and M. Wainwright, “High-dimensional analysis of semidefinite relaxations for sparse principal components,” *The Annals of Statistics*, vol. 37, no. 5B, pp. 2877–2921, 2009.
- [28] D. Paul and I. M. Johnstone, “Augmented sparse principal component analysis for high dimensional data,” *arXiv preprint arXiv:1202.1242*, 2012.